A fully automated immunoassay from whole blood on a disc†

Beom Seok Lee,[a] Jung-Nam Lee,[a] Jong-Myeon Park,[a] Jeong-Gun Lee,*[a] Suhyeon Kim,[a] Yoon-Kyoung Cho*[b] and Christopher Ko[a]

Received 17th November 2008, Accepted 4th February 2009
First published as an Advance Article on the web 5th March 2009
DOI: 10.1039/b820321k

A portable, disc-based, and fully automated enzyme-linked immuno-sorbent assay (ELISA) system is developed to test infectious diseases from whole blood. The innovative laser irradiated ferrowax microvalves and centrifugal microfluidics were utilized for the full integration of microbead-based suspension ELISA assays on a disc starting from whole blood. The concentrations of the antigen and the antibody of Hepatitis B virus (HBV), HBsAg and Anti-HBs respectively, were measured using the lab-on-a-disc (LOD). All the necessary reagents are preloaded on the disc and the total process of the plasma separation, incubation with target specific antigen or antibody coated microbeads, multiple steps of washing, enzyme reaction with substrates, and the absorbance detection could be finished within 30 minutes. Compared to the conventional ELISA, the operation time was dramatically reduced from over 2 hours to less than 30 minutes while the limit of detection was kept similar; *e.g.* the limit of detection of Anti-HBs tests were 8.6 mIU mL^{-1} and 10 mIU mL^{-1} for the disc-based and the conventional ELISA respectively.

1. Introduction

ELISA has been an indispensable tool in clinical diagnostics to quantify small concentrations of antibody or antigen in biological samples. However, common ELISA requires labor-intensive and time-consuming protocols involving multiple steps of incubation and washing. The automated ELISA systems used in clinical settings are rather large and expensive.[1–3]

Microfluidic platforms are advantageous because they use a smaller volume of reagents, have enhanced reaction efficiency and shorter reaction time due to larger surface-to-volume ratio and improved mass transport efficiency.[1–15] They are often simple to operate and less hazardous to use, and provide cheaper and portable analytical systems. Microchip-based ELISA studies showed that the amount of sample and reagents could be significantly reduced and the antigen-antibody reaction could take place much faster.[1–15] Employing microchannels results in larger surface-to-volume ratio and the improved mass transport efficiency.[1,15,16]

The use of microbeads as a surface binding platform further increases the surface area.[2–4,6,7,9–12,17] Microbeads could be used either in suspension assays or packed bead beds format. Packed bead beds could be formed in microfluidic chips by utilizing microfabricated structures such as weirs or pillars.[17] In flow-through type microfluidic chips using packed bead beds, the diffusion distances are substantially reduced and therefore enhanced surface-based bioassays were reported in broad applications from solid phase extractions to immuoassays.[6,18–23]

When the suspension assays rather than packed bead beds are utilized, it can be advantageous in the perspective of target sample delivery to the solid surfaces. However, suspension assays have not often been employed in microfluidic chips due to the difficulties associated with keeping the suspension state.

Disc-based immunoassays are an effective way to realize integrated analysis systems for point-of-care laboratory settings.[1,4,9,12,14,24,25] Though the examples of the disc-based immunoassays showed improved assay performances such as reduced amount of reagents and faster analysis time, it is the first time, to the best of our knowledge, a fully automated immuoassay starting from whole blood has been reported. Even though the plasma extraction from whole blood on a centrifugal platform itself is not a difficult problem,[26] a full integration of bioassays from whole blood has not been an easy task due to the limitation of the conventional hydrophobic or capillary valves.

In typical LOD systems,[1,4,9,12,14,24,25] the fluidic transfer is often controlled by spin speed. For example, the sequential transfer of reagents was accomplished by increasing spin speed step by step to realize the fully automated disc-based bioassays.[1,25] However, the plasma separation is often the first step in bioassays requiring relatively high spin speed which limits the number of following reaction steps.

Recently, we have demonstrated an innovative laser irradiated ferrowax microvalve (LIFM) that is based on the phase transition of ferrowax, paraffin wax embedded with 10 nm sized iron oxide

[a]*Bio & Health Group, Samsung Advanced Institute of Technology, P.O. Box 111, Suwon, 440-600, Korea. E-mail: biogun.lee@samsung.com; Fax: +82-13-280-8277; Tel: +82-31-280-6989*
[b]*UNIST San 194 Banyeon-ri, Eonyang-eup, Ulju-gun, Ulsan, 689-805, Korea. E-mail: ykcho@unist.ac.kr; Fax: +82-52-708-7010; Tel: +82-52-708-7010*

† Electronic supplementary information (ESI) available: Movie 1—the full process of ELISA on a disc starting from whole blood. The spin program is summarized in Table 1. The snapshot images are shown in Fig. 3. The details about the visualization on centrifugal microfluidics has been reported previously;[27,28] and Movie 2—the mixing of the microbeads on a centrifugal microfluidic device is investigated by the numerical simulation tool, Flow3D (Flow Science, Inc.). The movie shows the mixing pattern of microbeads inside the mixing chamber at the given experimental condition; maximum spin speed of 250 rpm, acceleration time of 0.1 second, duration time of 0.1 second, deceleration time of 0.1 second, and 1.74×10^4 microbeads. Temporal snapshot images of the bead mixing pattern and the fluid velocity inside the mixing chamber are shown in Fig. 4D. See DOI: 10.1039/b820321k

nanoparticles.[27,28] Laser light of relatively low intensity was able to melt the paraffin wax with the embedded iron oxide nanoparticles, whereas a high intensity laser beam alone could not melt the wax. Using the novel LIFM together with the pathogen specific magnetic particles, we could fully integrate the pathogen specific DNA extraction from whole blood on a portable lab-on-a-disc device.[27]

In this article, we report a fully automated lab-on-a-disc for immunoassays starting from whole blood. One hundred and fifty μL of whole blood, *i.e.* half of that required for the conventional ELISA, is applied directly to a disposable plastic disc containing reagents and buffers required for the immunoassays to detect Anti-HBs or HBsAg. As the disc is loaded into the portable blood analyzer, the total process of ELISA is automatically started. The portable analyzer is equipped with an optical detection module to measure the absorbances at 450 nm and 630 nm. The total process could be accomplished within 30 minutes without any manual interference and the assay results were as good as that of the conventional ELISA.

2. Materials and methods

2.1. Assay scheme and disc design

The reaction principle of the bead-based immunoassay to detect *e.g.* Anti-HBs on a disc is schematically shown in Fig. 1. The disc layout with the function of each chamber is shown in Fig. 1A. It has plasma separation channels, chambers containing substrate solution, washing buffer storage chambers, stopping solution chambers, mixing chambers, waste chambers, and detection chambers.

For rapid and versatile operation of multiple valves using a single laser diode, we have reported unique phase change based microvalves.[28] Utilizing the capillary forces in microchannels and the laser irradiation, the normally-open LIFM (NO-LIFM), the normally-closed LIFM (NC-LIFM), and the reversible LIFM were all possible.[28] As shown in Fig. 1A, the valves indicated with the numbers 3, 6, 9, and 12 are the NO-LIFM and all other valves are the NC-LIFM.[28] The valves are made of nanocomposite materials in which 10 nm-sized iron oxide nanoparticles are dispersed in paraffin wax. Using the mechanism of melting paraffin wax matrix with embedded nanoparticles by laser irradiation, the response time to operate the valve was very short, less than 1 sec.

HRP-conjugated detection antigen and polystyrene beads precoated with capture antigen are suspended in a commercially available conjugate dilution buffer (1× PBS + 1% BSA, GreenCross Co., Korea) and preloaded in the mixing chamber. The conjugate dilution buffer contains detergent, protein additives, magnesium and calcium salt, etc to reduce nonspecific binding of the conjugate to the plastic surface while maintaining HRP enzymatic activity.

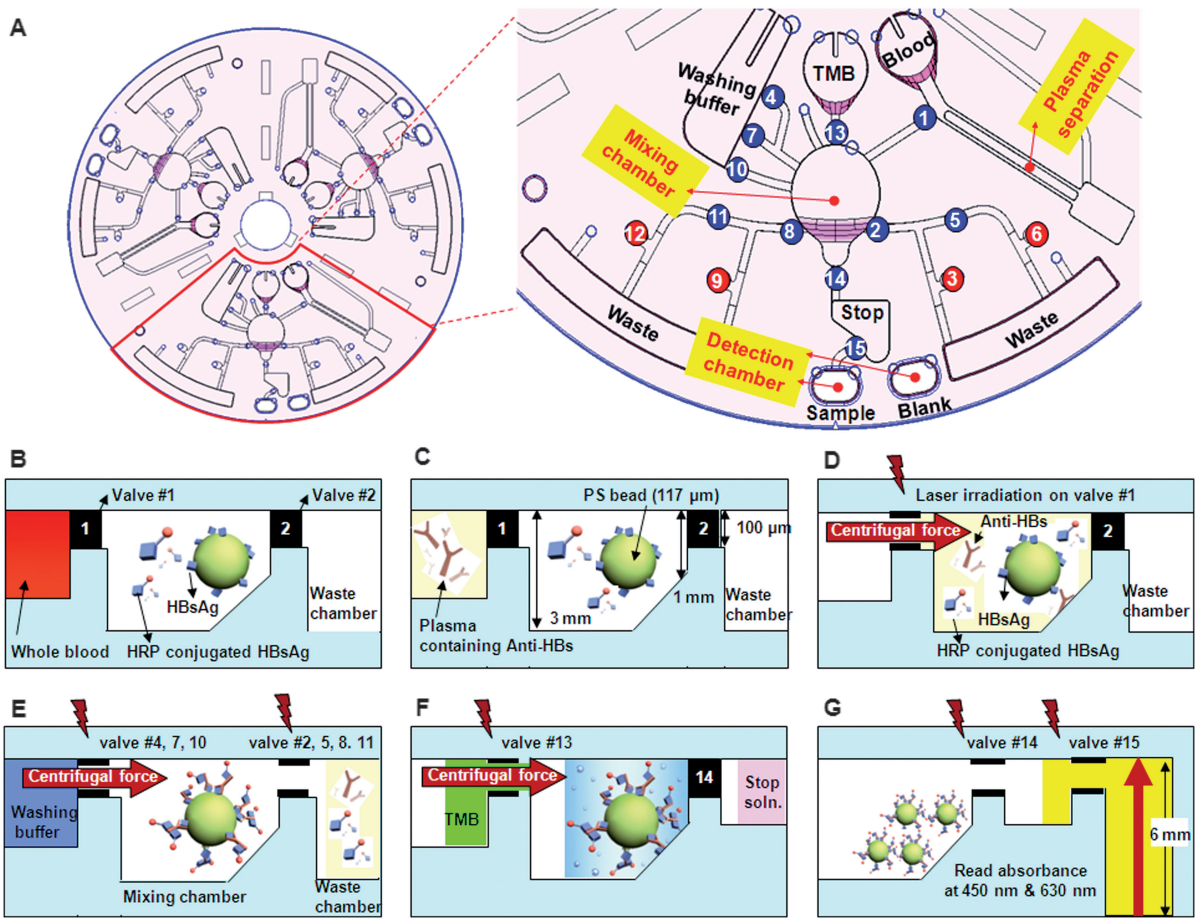

Fig. 1 (**A**) Disc design showing the detailed microfluidic layout and functions. The number indicates the order of the LIFM operation. (**B**–**G**) Schematic diagram of the reaction principle of the ELISA on a disc. The lightning symbols indicate the laser irradiation on the LIFM.

After introducing 150 μL of whole blood (Fig. 1B), the disc spins with the spin speed of 3600 rpm for 3 minutes to separate the plasma from whole blood sample (Fig. 1C). Upon laser irradiation at the valve # 1, 50 μL of the plasma is transferred into the mixing chamber (Fig. 1D). After incubation for 10 min, the plasma residue is removed through the valve # 2. After closing the valve # 3, the washing buffer is transferred into the mixing chamber by opening the valve # 4.

After washing the microbeads, the waste solution is removed to the waste chamber by opening the valve # 5 and the chamber is sealed by closing the valve # 6. After repeating the washing step for 2 more times by sequential operation of the valves from the valve # 7 to the valve # 12 (Fig. 1E), the washed beads are reacted with the TMB solution by opening the valve # 13 (Fig. 1F).

After 10 minutes, the reacted substrate is transferred into the chamber preloaded with the stopping solution by opening the valve # 14 (Fig. 1G). After mixing, the solution is transferred into the detection chamber by opening the valve # 15. Finally, the optical transmittance is measured at the detection chamber and the absorbance is calculated by comparing the transmittance measured at the blank chamber.

2.2. Instrumentation

As shown in Fig. 2A, a small sized blood analyzer (265 × 342 × 280 mm) has been developed for fully automated immunoassays from whole blood. It is comprised of a disc loader, a disc positioning and rotation controller, a laser position controller, an optical detection unit, a temperature controller, and a user interface controller (Fig. 2B).

Users can insert a disc through the disc loader. The disc can spin upto 5000 rpm with the acceleration of 3333 sec^{-2} and precisely positioned with the resolution of 0.09 degree using the main motor (23KM-249B, NMB tech. Japan).

The laser (BS808T3000FAC, Best Sources co. China) module is used to control the valve operation. The temperature is controlled at 37 ± 0.5 °C using a PID control algorithm and temperature sensor chip (LM92, National semiconductor).

For the absorbance detection, 2 photodiodes (S-1133-14, Hamamatsu) and the corresponding LEDs (450 and 630 nm) are used. The measured signal is amplified by a trans-impedance amplifier (OPA356, Texas instruments) and digitized by an analog to digital converter (ADS1258, Texas instruments).

2.3. Fabrication of LOD

As shown in Fig. 2C, a disc is composed of a top and bottom plate. These are injection molded plates made of PMMA (Plexiglas® 6N S000, Röhm GmbH) and the top plate has inlet holes. The top and bottom plates were bonded by using an UV adhesive (SSCP, Korea). In order to achieve good bonding characteristics, the UV adhesive was applied only in the bonding area by using a piezo-type dispenser (UJ200, UniJet Co) as shown in Fig. 2D.

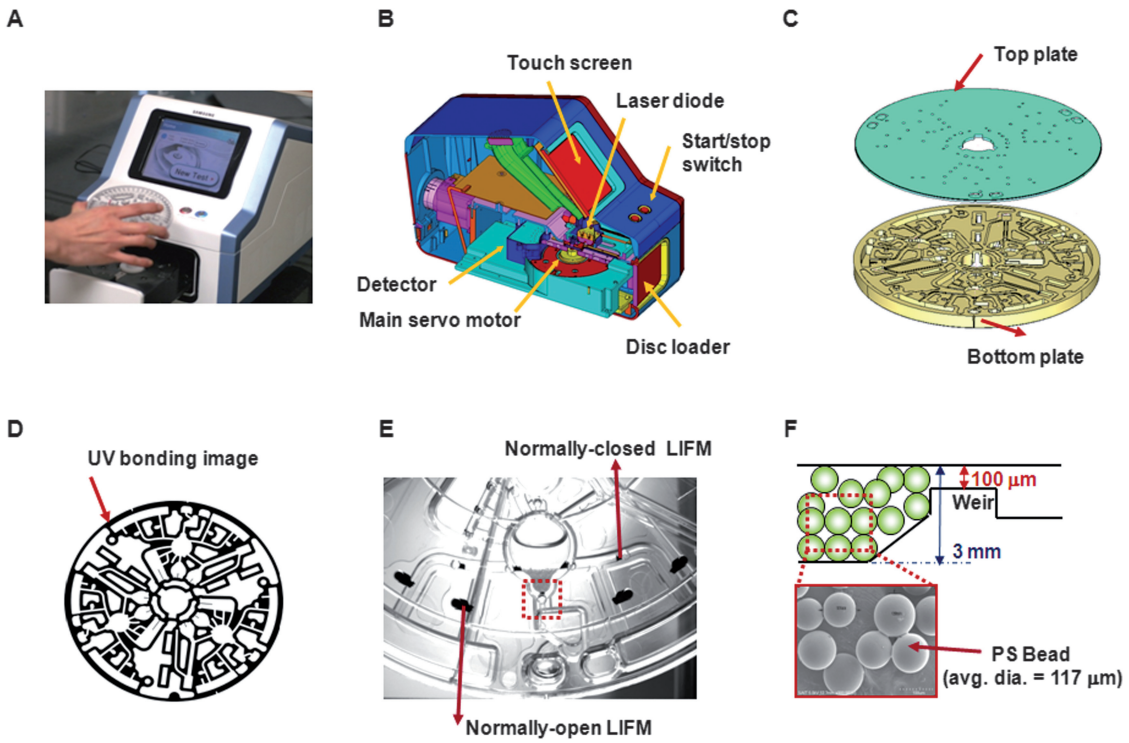

Fig. 2 (**A**) A photo image of the blood analyzer. (**B**) Schematic diagram showing the inside of the blood analyzer. A detector module is installed for the absorbance detection. (**C**) Top and bottom plate of the disc before the bonding. (**D**) An example of UV bonding image. The black area is where the UV adhesive is applied. (**E**) A photo image of the bonded disc after the valve formation. (**F**) A schematic diagram showing the side view of the mixing chamber (noted as red dotted square in part E). The PS beads are confined in the mixing chamber by the weir structure in the outlet of the mixing chamber.

The UV curing was done by applying an UV lamp (20 mW, Lichtzen, Korea) for 10 second after the two plates are aligned to face each other.

Fig. 2E shows a photo image of the bonded disc after loading the PS beads and the valves. The predetermined amount of PS beads suspension was injected into the mixing chamber and the inlet holes were sealed. The PS beads were confined in the mixing chamber by a weir structure (Fig. 2F) and could not be transferred to other chambers.

2.4. Reagents and materials

As capture proteins, recombinant HBsAg (20.00 μg mL^{-1} in Phosphate Buffered Saline (PBS), pH 7.0) and purified mouse monoclonal Anti-HBs (clone B4301, 18.75 μg mL^{-1} in PBS, pH 7.4) were used to detect Anti-HBs and HBsAg, respectively. Horseradish peroxidase (HRP) conjugated recombinant HBsAg and goat polyclonal Anti-HBs were used as detection proteins to detect Anti-HBs and HBsAg, respectively. The substrate was tetramethyl benzidine (TMB) in dimethyl sulfoxide (DMSO) and the washing solution was PBS with 1% Tween 20. The stopping solution was 1.6 N H_2SO_4. All of the above reagents were purchased from GreenCross Co. in Korea.

The carboxylated and aminated polystyrene beads (117 μm in diameter, BeadTech, Korea) were used to conjugate HBsAg and Anti-HBs, respectively. The protein immobilization procedure was based on the standard protocol suggested by Bang's lab.[29] In order to conjugate HBsAg on carboxylated microbeads, 0.1 M MES (2-(N-morpholino)ethanesulfonic acid, Sigma M3671) buffer with pH 6.07 and pH 7.78 were used for activation (15 min. at 25 °C) and conjugation (3 hr. at 25 °C). As an activation reagent, water soluble EDC (1-ethyl-3-(3-dimethylaminopropyl) carbodiimide hydrochloride, Pierce) was used. For the quenching step, the quenching solution is made from 35 mM hydroxylamine (Sigma 438227) as the primary amine source and 0.01% (w/v) BSA as a blocking material. The quenching step took 30 min. at 25 °C and was kept at 4 °C overnight.

For Anti-HBs conjugation, 0.125 % glutaraldehyde solution was used as an activation reagent. The amine functional group of polystyrene beads were activated into aldehyde group for 3 hours at room temperature. Then Anti-HBs conjugation on the activated beads was done in a coupling buffer (0.1 M Carbonate buffer, pH 9.5, Sigma) including Anti-HBs overnight at 4 °C. For stopping the conjugation step, 10 mg mL^{-1} sodium borohydride was used for 1 hr. After washing, the Anti-HBs conjugated beads were stored in a storage buffer (1× PBS + 1% Tween + 5% Casein, Sigma) at 4 °C, where 5% casein was used as a blocking material.

3. Results and discussion

3.1. Fully automated immunoassay on a disc

A fully integrated immunoassay disc containing all the reagents required to detect Anti-HBs or HBsAg is prepared. After 150 μL of whole blood is applied directly to a disposable plastic disc, the disc is inserted into the blood analyzer and the spin program shown in Table 1 is automatically started.

Table 1 Spin program

Spin No.	Speed (rpm)	Time (sec.)	Operation
1	3600	180	Plasma separation
2	2400	20	Transfer plasma into mixing chamber
3	+250∼−250	600	Mix beads, plasma & detection probe
4	2400	35	Remove residue to waste chamber
5	—	2	Close 1st waste channel
6	2400	20	Transfer 1st washing buffer (150 μL) to mixing chamber
7	+250∼−250	20	Mixing beads and washing buffer
8	2400	35	Remove 1st washed residue
9	—	2	Close 2nd waste channel
10∼17		170	Repeat 6∼9 twice for 2nd and 3rd washing step (each 100 μL)
18	2400	20	Transfer TMB to mixing chamber
19	+250∼−250	600	Mixing beads and TMB
20	2400	20	Transfer to stopping solution chamber
21	+250∼−250	20	Mixing with stopping solution
22	2400	20	Transfer to detection chamber
23	—	20	Detection

As the first spin program, the disc is rotated with the spin speed of 3600 rpm for 3 minutes to separate plasma from the whole blood (Fig. 3A). It usually takes only less than a minute to separate the plasma from blood samples. However, it was rotated for 3 minutes to deal with various kinds of blood samples. After the plasma sample is transferred into the mixing chamber (Fig. 3B), the disc is rotated in the mixing mode to promote the binding reaction (Fig. 3C). The spin condition for the rapid mixing is discussed in detail in the next section.

After the incubation, the sample residue is removed by opening the valve #2 and the mixing chamber is sealed again by closing the valve #3. When the sample residue is decanted to the waste chamber, the microbeads are packed in the lower region of the mixing chamber.

In order to wash the microbeads, 150 μL of washing buffer is transferred into the mixing chamber (Fig. 3D). As the disc spins at the mixing mode, the sedimented microbeads are suspended again and the microbeads are washed effectively. After the washing step, the washing buffer residue is removed to the waste chamber by opening the valve #5 and the mixing chamber is sealed by closing the valve #6. After repeating the washing step 2 more times, 65 μL of TMB solution is transferred into the mixing chamber (Fig. 3E).

After incubation for 10 minutes, the final solution is transferred into the stopping solution (Fig. 3F). Finally, the absorbance is measured at 450 nm and 630 nm through the detection chamber and the concentration of Anti-HBs or HBsAg are displayed on the screen of the blood analyzer. The total process is finished within 30 minutes without an additional manual step (see Movie 1 in the ESI for the full process†).

As shown in Fig. 1, the disc has 3 identical units that can be used for 3 independent immunoassays. We have used only one unit for the clear demonstration purpose. However, 3 units could be run simultaneously and the total operation time was less than 50 minutes to finish 3 immunoassays that were composed of HBsAg unit, Anti-HBs unit and a control unit respectively.

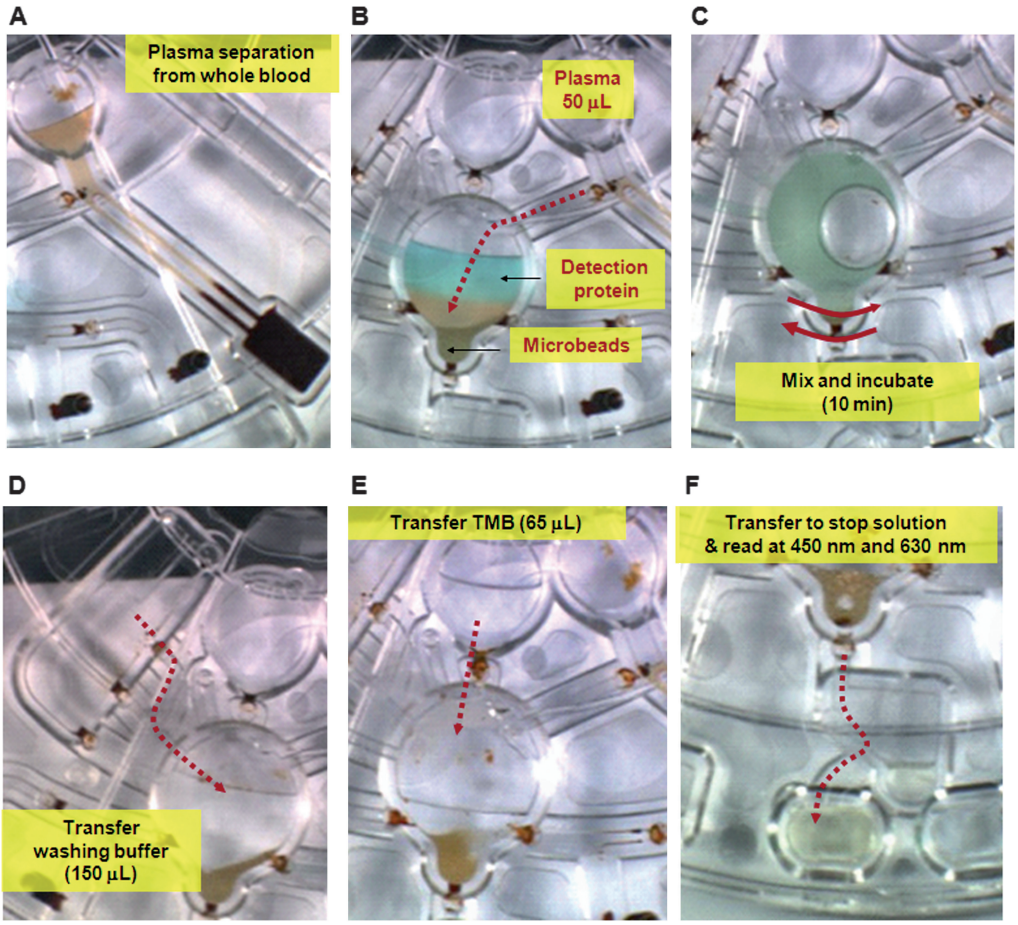

Fig. 3 CCD images captured at each spin step using the spin program shown in Table 1. (**A**) An image captured after spin no. 1 shows that the plasma is separated from whole blood. (**B**) An image captured after spin no. 2 shows the sample transferred into the mixing chamber containing microbeads. (**C**) An image captured during spin no. 3 shows the mixing of microbeads with the samples. (**D**) An image captured after spin no. 6 shows that 150 μL of washing buffer is transferred into the mixing chamber. (**E**) An image captured after spin no. 18 shows that the substrate is transferred into the mixing chamber. (**F**) An image captured after spin no. 22 shows the final state of the reaction.

3.2. Microbeads-based suspension assay on a disc

In this article, microbead-based suspension assays are integrated on a disc for the first time to the best of our knowledge. The advantages of using microbeads on a centrifugal microfluidic device is the following. First, our microbeads have 50 times larger surface to volume ratio compared to the common ELISA microplates. Second, as shown in Fig. 3C, the microbeads are vigorously mixed during the binding reaction time by repeating the disc spin in clockwise and counter-clockwise direction. This convective mixing of microbeads and the reagents could reduce diffusion length between proteins and the solid surface of the beads. As a result, the incubation time could be dramatically reduced.

In a previous article, we utilized magnetic force to recover the suspension state from the packed bed of magnetic microparticles.[27] In this article, however, we utilized regular polystyrene (PS) microbeads instead of magnetic particles to reduce the assay costs. One of the difficulties associated with PS microbeads on a disc was to recover the suspension state from the packed bed state after spining the disc at high spin speed.

When the disc is repetitively rotated in clockwise and counter clockwise direction, it was observed that the sedimented beads are suspended again within 1 second as shown in Fig. 4A. The optimum mixing condition was experimentally obtained when the disc repetitively spins clockwise and counter clockwise with the maximum spin speed of $\pm$ 250 rpm at the acceleration time of 0.1 second, the duration time of 0.1 second and the deceleration time of 0.1 second. If the spin speed is too high or the disc spins too long, the beads were sedimented and it was not easy to recover the suspension state. The acceleration and the number of the change in spin direction were the key parameters to achieve the rapid mixing.

The mixing of the microbeads on a centrifugal microfluidic device is investigated by the numerical simulation tool, Flow3D (Flow Science, Inc.). It is a highly complex 3-dimensional mixing problem because it is the particle-fluid couple case in the non-inertial reference frames. Fig. 4B shows representative spin profiles of the simulation conditions. In this paper, the effect of maximum spin speed on the mixing time required to recover the suspension state is investigated while other parameters are fixed. For example, the acceleration time, the deceleration time, and the

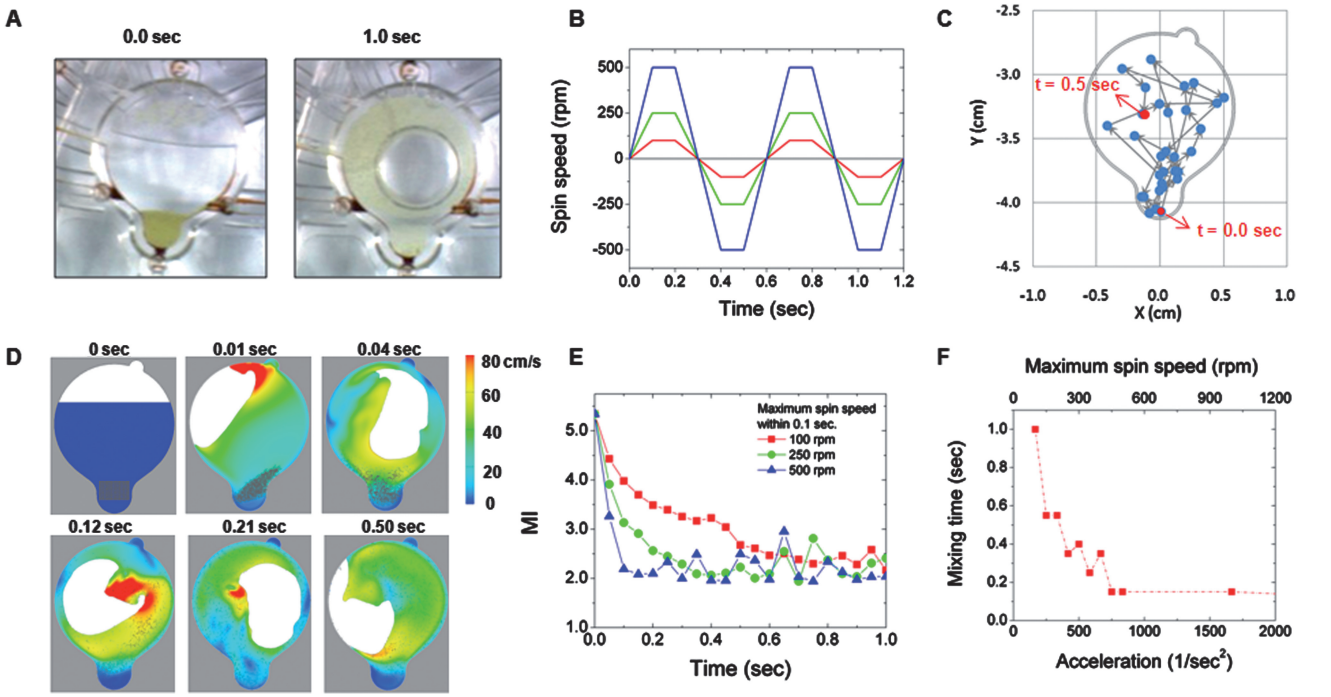

Fig. 4 Investigation of bead mixing inside the mixing chamber by numerical analysis, (**A**) CCD images obtained before and 1.0 second after the mixing mode operation. (**B**) A representative mixing mode spin program. The spin program is repeated during the incubation time. (**C**) Particle trajectory of one bead initially located at the lowest region of the mixing chamber for 0.6 second. (**D**) Temporal snapshot images of the bead mixing pattern and the fluid velocity inside the mixing chamber. (**E**) Mixing index (MI) along the elapsed time at various mixing conditions. (**F**) The effect of the acceleration on the time to reach the uniformly mixed state.

duration time are fixed at 0.1 second and the number of the change in spin direction is also fixed.

First, we investigated the temporal mixing pattern of microbeads inside the mixing chamber at the given experimental condition; maximum spin speed of 250 rpm, acceleration time of 0.1 second, duration time of 0.1 second, deceleration time of 0.1 second, and 1.74×10^4 microbeads.

Fig. 4C shows a particle tracking image during the first 0.5 seconds. A particle noted as a red circle is initially located at the lowest region and the location of the bead at each time step of 0.02 seconds is represented as blue circles. The microbead escapes quickly from the starting lower position and travels throughout the whole mixing chamber.

Fig. 4D shows the successive images up to 0.5 second with the contour of fluid velocity, where the 2D images in the horizontal x-y plane are extracted from the center of z axis in the 3D domain (see Movie 2 in the ESI for the full process of bead mixing†). The results show that a uniformly mixed state could be achieved within 0.5 second. It was also observed that the void inside of the mixing chamber accelerates the mixing of microbeads inside the fluid region of the mixing chamber.

In order to have a quantitative measure to represent the mixing state, we defined the mixing index (MI).[30]

$$\mathrm{MI} = \frac{1}{c_f} \times \sqrt{\frac{1}{V_{total}} \sum_i (c_i - c_f)^2 V_i}$$

where i is the index of the cell which is a computationally discretized unit in the mixing chamber, c_f is the volume ratio of the total bead to the total fluid inside the mixing chamber, c_i is the volume ratio of the bead to the fluid in the i^{th} cell, V_{total} is the total fluid volume in the mixing chamber, and V_i is the fluid volume in the i^{th} cell.

In Fig. 4E, the mixing index is plotted as the function of the elapsed time at different spin conditions. It shows that MI decreases faster at higher maximum spin speed (*i.e.* higher acceleration because the acceleration time was fixed at 0.1 second). The minimum value of the MI is almost 2 when the beads are uniformly mixed. The MI value is fluctuated as time goes on because the mixing of beads inside the mixing chamber reaches the unsteady equilibrium state. Furthermore, the degree of oscillation of MI becomes larger as the rotation speed increases. In our experimental condition, *i.e.* the maximum spin speed of 250 rpm, the time to reach the uniformly mixed state was 0.35 second. Fig. 4F shows the dramatic decrease of the mixing time to reach the uniformly mixed state as the maximum spin speed (*i.e.* acceleration) increases.

3.3. Comparison with manual ELISA

In Fig. 5, the calibration curves obtained by using the fully automated LOD are shown. For the calibration curves, the standard samples from an ELISA kit (Genedia GreenCross Co., Korea) were used because it was easier to obtain quantitative comparison in a broad range of the sample concentration. The standard sample was diluted using the normal human serum (Linear Chemicals, Spain). Therefore, we believe the calibration

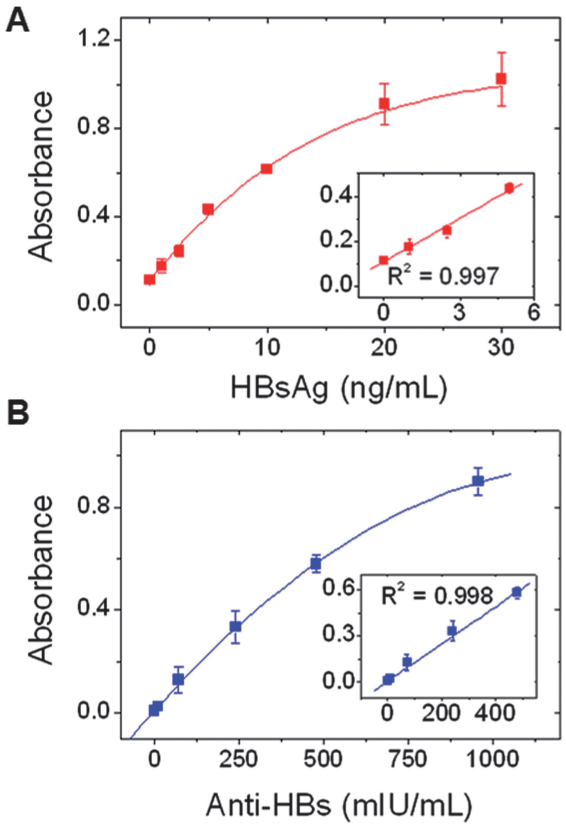

Fig. 5 Absorbance measured by the blood analyzer. Calibration curves of (**A**) HBsAg and (**B**) Anti-HBs detection using the fully automated lab-on-a-disc. Each data point is the average of the 6 measurements obtained by 6 separate discs. The lines are a polynomial curve fitting. The inset shows the linear dynamic range.

curves are similar to that can be achieved using whole blood samples.

In Table 2, the LOD based immunoassay results are compared with the data obtained by a conventional ELISA kit. The disc utilizes microbeads where the surface to volume ratio is 50 times larger than the microplate of the manual ELISA kit. The operation time was less than 30 minutes as compared to over 2 hours.

Table 2 Comparison of the performance specifications of the assays measured by lab-on-a-disc and a conventional ELISA[a]

	Disc	ELISA
HBsAg		
Operation Time (min)	30	>120
Sample Volume (μL)	50	100
Linear Dynamic Range (ng/mL)	0.51∼5	0.56∼2.5
Limit of Detection (ng/mL)	0.51	0.56
Anti-HBs		
Operation Time (min)	30	>90
Sample Volume (μL)	50	100
Liner Dynamic Range (mIU/mL)	8.6∼480	10∼150
Limit of Detection (mIU/mL)	8.6	10

[a] Calibration curves were obtained by using the standard samples provided by an ELISA kit (Genedia GreenCross Co., Korea) because sample ranges were broader than the venous whole blood samples.

The plasma sample volume of the disc was half that required in ELISA; 50 μL vs 100 μL.

The linear dynamic ranges both for HBsAg and Anti-HBs are about two-fold wider than those obtained in ELISA with similar R^2. Based on the definition of LOD commonly used in conventional ELISA kits,[31] the limit of detection (LOD) was calculated 2 times the standard deviation of the signal measured with the negative control samples. The LODs of HBsAg and Anti-HBs are 0.51 ng/mL and 8.6 mIU/mL, respectively, which are comparable to those obtained with the ELISA kits.

A large scale clinical evaluation is under investigation. Meanwhile, the tests done by using one of the author's venous blood showed good correlation with the results measured at a hospital (Architect i2000, Samsung Medical Center, Korea). The concentration of the Anti-HBs measured by the proposed blood analyzer and at the hospital was 1096 ± 97 mIU/mL and 1000 mIU/mL, respectively.

Conclusions

A portable and fully automatic immunoassay system is developed. A microbead-based immunoassay starting from whole blood is fully integrated on a disc utilizing centrifugal forces and the innovative laser irradiated ferrowax microvalves. The optimum spin condition to recover the suspension state from the sedimented state as well as to achieve rapid mixing was investigated in order to utilize PS microbeads on a centrifugal microfluidic platform.

As a model study, HBsAg and Anti-HBs tests were integrated on a disc. By using the disc with preloaded reagents and fully automated disc operation system, laborious tasks were eliminated and the assay time was remarkably reduced from 2 hr to 30 minutes. Moreover, no special skills are necessary. Even though only Anti-HBs and HBsAg detection was demonstrated here, other ELISA protocols can be easily applied to the same kinds of disc.

Acknowledgements

This research was sponsored in part by the Ministry of Commerce, Industry and Energy (MOCIE) of the Republic of Korea under the next generation new technology development project (00008069) through the Bio Device Research Lab at the Samsung Advanced Institute of Technology (SAIT).

References

1 S. Lai, S. Wang, J. Luo, L. J. Lee, S.-T. Yang and M. J. Madou, *Anal. Chem.*, 2004, **76**, 1832–1837.
2 K. Sato, M. Yamanaka, T. Hagino, M. Tokeshi, H. Kimura and T. Kitamori, *Lab Chip*, 2004, **4**, 570–575.
3 M. Herrmann, T. Veres and M. Tabrizian, *Anal. Chem.*, 2008, **80**, 5160–5167.
4 N. Honda, U. Lindberg, P. Andersson, S. Hoffmann and H. Takei, *Clinical Chemistry*, 2005, **51**, 1955–1961.
5 N. Christodoulides, M. Tran, P. N. Floriano, M. Rodriguez, A. Goodey, M. Ali, D. Neikirk and J. T. McDevitt, *Anal. Chem.*, 2002, **74**, 3030–3036.
6 Y. Murakami, T. Endo, S. Yamamura, N. Nagatani, Y. Takamura and E. Tamiya, *Analytical Biochemistry*, 2004, **334**, 111–116.
7 W.-T. Liu, L. Zhu, Q.-W. Qin, Q. Zhang, H. Feng and S. Ang, *Lab Chip*, 2005, **5**, 1327–1330.

8 T. Endo, A. Okuyama, Y. Matsubara, K. Nishi, M. Kobayashi, S. Yamamura, Y. Morita, Y. Takamura, H. Mizukami and E. Tamiya, *Analytica Chimica Acta*, 2005, **531**, 7–13.
9 L. Riegger, J. Steigert, M. Grumann, S. Lutz, G. Olofsson, M. Khayyami, W. Bessler, K. Mittenbühler, R. Zengerle and J. Ducrée, *Micro TAS 2006*, Tokyo, Japan, 2006.
10 M. Herrmann, T. Veres and M. Tabrizian, *Lab Chip*, 2006, **6**, 555–560.
11 D. Holmes, J. K. She, P. L. Roach and H. Morgan, *Lab Chip*, 2007, **7**, 1048–1056.
12 L. Riegger, M. Grumann, T. Nann, J. Riegler, O. Ehlert, W. Bessler, K. Mittenbühler, G. Urban, L. Pastewka, T. Brenner, R. Zengerle and J. Ducrée, *Sensors and Actuators A*, 2006, **126**, 455–462.
13 M. C. Peoples and H. T. Karnes, *Anal. Chem.*, 2008, **80**, 3853–3858.
14 J. Tamarit-López, S. Morais, R. Puchades and Á. Maquieira, *Analytica Chimica Acta*, 2008, **609**, 120–130.
15 S. Cesaro-Tadic, G. Dernick, D. Juncker, G. Buurman, H. Kropshofer, B. Michel, C. Fattinger and E. Delamarche, *Lab Chip*, 2004, **4**, 563–569.
16 A. Lionello, J. Josserand, H. Jensen and H. H. Girault, *Lab Chip*, 2005, **5**, 254–260.
17 E. Verpoorte, *Lab Chip*, 2003, **3**, 60N–68N.
18 K. Sato, M. Tokeshi, T. Odake, H. Kimura, T. Ooi, M. Nakao and T. Kitamori, *Anal. Chem*, 2000, **72**, 1144–1147.
19 K. Sato, M. Tokeshi, H. Kimura and T. Kitamori, *Anal. Chem.*, 2001, **73**, 1213–1218.
20 H. Andersson, W. van der Wijngaart and G. Stemme, *Electrophoresis*, 2001, **22**, 249–257.
21 R. D. Oleschuk, L. L. Shultz-Lockyear, Y. Ning and D. J. Harrison, *Anal. Chem.*, 2000, **72**, 585–590.
22 R. D. Oleschuk, A. B. Jemere, L. L. Schultz-Lockyear, F. Fajuyigbe and D. J. Harrison, *Micro TAS 2000*, Dordrecht, The Netherlands, 2000.
23 A. Russom, A. Ahmadian, H. Andersson, P. Nilsson and G. Stemme, *Electrophoresis*, 2003, **24**, 158–161.
24 J. V. Zoval and M. J. Madou, *Proceedings of the IEEE*, 2004, **92**, 140–153.
25 L. G. Puckett, E. Dikici, S. Lai, M. Madou, L. G. Bachas and S. Daunert, *Anal. Chem.*, 2004, **76**, 7263–7268.
26 S. Haeberle, T. Brenner, R. Zengerle and J. Ducrée, *Lab Chip*, 2006, **6**, 776–781.
27 Y.-K. Cho, J.-G. Lee, J.-M. Park, B.-S. Lee, Y. Lee and C. Ko, *Lab Chip*, 2007, **7**, 565–573.
28 J.-M. Park, J.-G. Lee, Y.-K. Cho, B.-S. Lee and C. Ko, *Lab Chip*, 2007, **7**, 557–564.
29 L. B. Bangs and M. Meza, *IVD Technology Magazine*, 1995.
30 A. D. Stroock, S. K. W. Dertinger, A. Ajdari, I. Mezic, H. A. Stone and G. M. Whitesides, *Science*, 2002, **295**, 647–651.
31 *TSH kit inserts (product number 11731459, Roche diagnostics)*, 2006.